Poroelastic response of a functionally graded hollow cylinder under an asymmetric loading condition

Tuan Nguyen-Sy, Minh-Ngoc Vu, Trung-Kien Nguyen, Anh-Dung Tran-Le, Minh-Quan Thai, Thoi-Trung Nguyen

Tuan Nguyen-Sy · Minh-Ngoc Vu · Trung-Kien Nguyen · Anh-Dung Tran-Le · Minh-Quan Thai · Thoi-Trung Nguyen

Poroelastic response of a functionally graded hollow cylinder under an asymmetric loading condition

Abstract This paper aims to develop semi-analytical results of the poromechanical fields in a hollow cylinder subjected to an asymmetric loading condition. The poroelastic properties of the hollow cylinder vary in the radial direction. The heterogeneous hollow cylinder is approximated by a multilayer structure in which each cylindrical layer is assumed to be homogeneous. The analytical results of the poromechanical field are first established in the transformed Laplace space, and then the ones in time space are obtained by the inverse Laplace transformation. They are perfectly in coherence with existent results in the literature that were developed for the homogeneous and the heterogeneous cases at the steady state regime. Sensitivity analysis shows a significant effect of the radial variations of the poroelastic properties on the response of the hollow cylinder.

Keywords Poroelastic · Functionally graded material · Hollow cylinder · Fluid diffusion · Asymmetric loading

Abbreviations

σ, Σ	Stress
ε, E	Strain
u, U	Displacement
p, P	Pore pressure
ζ, Z	Fluid exchange
q, Q	Fluid flow rate

T. Nguyen-Sy (✉) · T.-T. Nguyen
Division of Construction Computation, Institute for Computational Science, Ton Duc Thang University, Ho Chi Minh City, Vietnam
e-mail: nguyensytuan@tdtu.edu.vn

T. Nguyen-Sy · T.-T. Nguyen
Faculty of Civil Engineering, Ton Duc Thang University, Ho Chi Minh City, Vietnam

M.-N. Vu
Institute of Research and Development, Duy Tan University, Danang 550000, Vietnam

M.-N. Vu
Faculty of Natural Sciences, Duy Tan University, Danang 550000, Vietnam

T.-K. Nguyen · M.-Q. Thai
Research and Application Center for Technology in Civil Engineering, University of Transport and Communications, 3 Cau Giay, Dong Da Hanoi, Vietnam

A.-D. Tran-Le
Laboratoire Des Technologies Innovantes, Université de Picardie, Jules Verne Avenue des Facultés, 80025 Amiens Cedex 1, France

$\overline{x}$	Laplace's transform of a certain variable x
t	Time
s	Laplace's variable
r and θ	Cylindrical coordinates
H	In-plane drained compressional stiffness
G	In-plane shear modulus
M	Biot's modulus
b	Biot's coefficient
κ	Permeability
c	Diffusion coefficient
N	Number of layer
k and (k)	Index and exponent stand for kth layer
in and out	Indexes stand for the inner and outer faces of the whole hollow cylinder
I_1, I_2, K_1, K_2	Modified Bessel functions of the first and second kinds
m_1, m_2 and m_3	Coefficients defining the radial variations of the poroelastic properties

1 Introduction

Mechanical behavior of a hollow cylinder is an important research subject because of a large variety of related applications in many domains: petroleum wellbore drilling, tunnel excavation, cortical bone, aerospace, etc. [1–3]. Analytical results for an elastic homogeneous hollow cylinder can be found in most of the mechanical books. They can be obtained by solving the Navier's equation that is a second-order differential equation of the displacement. Analytical and semi-analytical results were also developed for the many more complex problems: homogeneous poroelastic borehole [6], heterogeneous elastic hollow cylinder [7, 8], or thermoelastic heterogeneous hollow cylinder at steady state regime [9, 10], just to cite a few. Recently, Nguyen-Sy et al. [11] have developed semi-analytical results for the transient diffusion of fluid through a heterogeneous poroelastic hollow cylinder subjected to a plane strain axisymmetric loading. However, the results for a functionally graded poroelastic hollow cylinder subjected to a shear loading do not exist yet in the literature.

The numerical simulation can be considered for such problem. However, it is important to derive analytical or semi-analytical results to benchmark the numerical codes. Also, analytical results can be considered for sensitivity/reliability tests of the related parameters (material properties, geometry, etc.) thanks to their negligible simulation time compared to the numerical method.

This paper aims to provide semi-analytical results of a functionally graded poroelastic hollow cylinder subjected to an asymmetric loading condition. It is organized as follows: first the theoretical basis of the model is presented. Second, semi-analytical results in Laplace space are derived. They are validated against existing results of simplified cases: a homogeneous borehole; and a heterogeneous case at the steady state fluid flow regime. Third, a sensitivity analysis is presented to clarify the effect of the radial variation of the poroelastic properties on the shearing response of the hollow cylinder. Concluding remark and Appendix 1 are given at the end of the paper.

2 Theoretical basis

2.1 Governing equations

Let us consider a poroelastic functionally graded hollow cylinder in which the poroelastic properties vary radially. A pure shear loading is applied on the inner boundary of the hollow cylinder as [6, 7]

$$\sigma_{\text{in}} = -p_0 \cos 2\theta; \tau_{\text{in}} = p_0 \sin 2\theta \tag{1}$$

where σ_{in} is the radial traction and τ_{in} is the shear stress on the inner boundary of the hollow cylinder. The poromechanical response obeys the Biot's poroelastic theory [4, 12], and fluid flow is described by the Darcy's law. It is approximated by a multilayer cylinder in which each cylindrical shell is assumed to be homogeneous (Fig. 1).

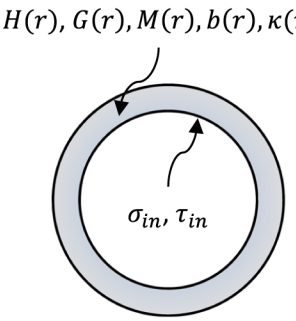

Fig. 1 Multilayer hollow cylinder under a pure shear loading

The poroelastic constitutive law relates the radial, tangent and shear stresses $\sigma_{rr}^{(k)}, \sigma_{\theta\theta}^{(k)}, \sigma_{r\theta}^{(k)}$ the pore pressure p_k, the fluid exchange ζ_k and the radial, tangent and shear strains $\varepsilon_{rr}^{(k)}, \varepsilon_{\theta\theta}^{(k)}, \varepsilon_{r\theta}^{(k)}$ in the kth layer as [5]

$$\sigma_{rr}^{(k)} + b_k p_k = H_k \varepsilon_v^{(k)} - 2G_k \varepsilon_{\theta\theta}^{(k)} \tag{2}$$

$$\sigma_{rr}^{(k)} - \sigma_{\theta\theta}^{(k)} = 2G_k\left(\varepsilon_{rr}^{(k)} - \varepsilon_{\theta\theta}^{(k)}\right); \sigma_{r\theta}^{(k)} = 2G_k \varepsilon_{r\theta}^{(k)} \tag{3}$$

$$p_k = M_k\left(\zeta_k - b_k \varepsilon_v^{(k)}\right) \tag{4}$$

where $\varepsilon_v^{(k)}$ is the volumetric strain in the kth layer that can be expressed in the plane strain condition as: $\varepsilon_v^{(k)} = \varepsilon_{rr}^{(k)} + \varepsilon_{\theta\theta}^{(k)}$; the in-plane drained compressional stiffness and the in-plane shear modulus of the kth layer are noted by H_k and G_k, respectively. The Biot's modulus and the in-plane Biot's coefficient are noted by M_k and b_k. The index k and the exponent (k) denote the properties and the poromechanical fields within the kth layer.

The radial and tangent fluid flow rate $q_r^{(k)}$ and $q_\theta^{(k)}$ at any point in the kth cylindrical shell are related to the pore pressure via the Darcy's law as

$$q_r^{(k)} = -\kappa_k \frac{\partial p_k}{\partial r}; q_\theta^{(k)} = -\kappa_k \frac{1}{r}\frac{\partial p_k}{\partial \theta} \tag{5}$$

where κ_k is the permeability that is the ratio between the intrinsic permeability of the kth layer and the fluid dynamic viscosity; r is the radial coordinate that is the distance from the considering point to the center of the hollow cylinder. The combination of the Darcy's law and the fluid mass conservation leads to the following diffusion equation [6]

$$\frac{\partial^2 \zeta_k}{\partial r^2} + \frac{1}{r}\frac{\partial \zeta_k}{\partial r} + \frac{1}{r^2}\frac{\partial^2 \zeta_k}{\partial \theta^2} = \frac{1}{c_k}\frac{\partial \zeta_k}{\partial t} \tag{6}$$

where c_k is the fluid diffusion coefficient of the kth layer that is related to its poroelastic properties as

$$c_k = \frac{\kappa_k M_k H_k}{H_k + M_k b_k^2} \tag{7}$$

The radial, tangent and shear strains are related to the radial and tangent displacements $u_r^{(k)}$ and $u_\theta^{(k)}$ by

$$\varepsilon_{rr}^{(k)} = \frac{\partial u_r^{(k)}}{\partial r}; \varepsilon_{\theta\theta}^{(k)} = \frac{1}{r}\frac{\partial u_\theta^{(k)}}{\partial \theta} + \frac{u_r^{(k)}}{r}; \varepsilon_{r\theta}^{(k)} = \frac{1}{2}\left(\frac{\partial u_\theta^{(k)}}{\partial r} - \frac{u_\theta^{(k)}}{r} + \frac{1}{r}\frac{\partial u_r^{(k)}}{\partial \theta}\right) \tag{8}$$

and the stress balance condition is

$$\frac{\partial \sigma_{rr}^{(k)}}{\partial r} + \frac{1}{r}\frac{\partial \sigma_{r\theta}^{(k)}}{\partial \theta} + \frac{\sigma_{rr}^{(k)} - \sigma_{\theta\theta}^{(k)}}{r} = 0 \tag{9}$$

Also, it will be useful to introduce a variable $\omega_z^{(k)}$ that is a component of the rotation vector of the displacement field [5]

$$\omega_z^{(k)} = \frac{1}{2}\left(\frac{\partial u_\theta^{(k)}}{\partial r} + \frac{u_\theta^{(k)}}{r} - \frac{1}{r}\frac{\partial u_r^{(k)}}{\partial \theta}\right) \tag{10}$$

The poroelastic coupling problem is not developed directly from the governing Eqs. (2), (3), (4), (8) and (9). It will be demonstrated in the following of the paper that it is more convenient to combine these relations after the cosine and sinus transformations. Indeed, the complexity related to the tangent variable θ can be avoided by that technique.

2.2 Parameters

There are five hydro-mechanical properties for each layer: κ_k, H_k, G_k, b_k and M_k. So, there are $5N$ parameters to fully describe the whole N-layers heterogeneous porous medium. In addition to the fluid diffusion coefficient c_k, some alternative poroelastic parameters will be also considered in this paper:

$$\beta_k = \kappa_k\sqrt{\frac{s}{c_k}}; \delta_k = \frac{b_k}{H_k}\sqrt{\frac{c_k}{s}}; \theta_k = \frac{2b_kG_k}{H_k} \tag{11}$$

where s is the Laplace transform variable.

2.3 Cosine and sinus transformations

The combination of Eqs. (2) to (9) forms the complete governing equation system of the problem. They can be simplified by considering the following cosinus and sinus transformations [6, 7]

$$p = P\cos 2\theta; q_r = Q_r\cos 2\theta; q_\theta = Q_\theta \sin 2\theta \tag{12}$$

$$u_r = U_r\cos 2\theta; u_\theta = U_\theta \sin 2\theta \tag{13}$$

$$\varepsilon_{rr} = E_{rr}\cos 2\theta; \varepsilon_{\theta\theta} = E_{\theta\theta}\cos 2\theta; \varepsilon_{r\theta} = E_{r\theta}\sin 2\theta \tag{14}$$

$$\sigma_{rr} = \Sigma_{rr}\cos 2\theta; \sigma_{\theta\theta} = \Sigma_{\theta\theta}\cos 2\theta; \sigma_{r\theta} = \Sigma_{r\theta}\sin 2\theta \tag{15}$$

and

$$\varepsilon_v = E\cos 2\theta; \frac{c}{\kappa}\zeta = Z\cos 2\theta; \omega_z = W\sin 2\theta \tag{16}$$

where the index k and the exponent (k) that stand for kth layer were omitted to simplify the expressions. Using these sinus and cosine transformations, the diffusion Eq. (6) can be simplified to

$$\frac{\partial^2 Z_k}{\partial r^2} + \frac{1}{r}\frac{\partial Z_k}{\partial r} - \frac{4}{r^2}Z_k = \frac{1}{c}\frac{\partial Z_k}{\partial t} \tag{17}$$

The Darcy law becomes

$$Q_r^{(k)} = -\kappa_k\frac{\partial P_k}{\partial r}; Q_\theta^{(k)} = 2\kappa_k\frac{P_k}{r} \tag{18}$$

The relationship between the strains, the rotation coefficient and the displacements (Eqs. (8) and (10)) can be also simplified to

$$E_{rr}^{(k)} = \frac{\partial U_r^{(k)}}{\partial r}; E_{\theta\theta}^{(k)} = 2\frac{U_\theta^{(k)}}{r} + \frac{U_r^{(k)}}{r}; E_{r\theta}^{(k)} = \frac{1}{2}\left(\frac{\partial U_\theta^{(k)}}{\partial r} - \frac{U_\theta^{(k)}}{r} - 2\frac{U_r^{(k)}}{r}\right) \tag{19}$$

and

$$E_k = \frac{\partial U_r^{(k)}}{\partial r} + 2\frac{U_\theta^{(k)}}{r} + \frac{U_r^{(k)}}{r}; W_k = \frac{1}{2}\left(\frac{\partial U_\theta^{(k)}}{\partial r} + \frac{U_\theta^{(k)}}{r} + 2\frac{U_r^{(k)}}{r}\right) \tag{20}$$

The stress balance condition and the poroelastic constitutive equations are transformed to

$$\frac{\partial \Sigma_{rr}^{(k)}}{\partial r} + \frac{2\Sigma_{r\theta}^{(k)}}{r} + \frac{\Sigma_{rr}^{(k)} - \Sigma_{\theta\theta}^{(k)}}{r} = 0 \tag{21}$$

and

$$\Sigma_{rr}^{(k)} + b_k P_k = H_k E_k - 2G_k E_{\theta\theta}^{(k)} \tag{22}$$

$$\Sigma_{rr}^{(k)} - \Sigma_{\theta\theta}^{(k)} = 2G_k\left(E_{rr}^{(k)} - E_{\theta\theta}^{(k)}\right); \Sigma_{r\theta}^{(k)} = 2G_k E_{r\theta}^{(k)} \tag{23}$$

$$P_k = M_k\left(\frac{\kappa_k}{c_k} Z_k - b_k E_k\right) \tag{24}$$

2.4 The poromechanical fields in each cylindrical shell

Equations (2) to (9) can be combined to obtain a diffusion equation of Z_k that can be transformed into a differential equation of $\overline{Z}_k$ in the Laplace transform space. The notation $\overline{x}$ stands for the Laplace transformation of a certain variable x. It is convenient to define a vector of the solutions as

$$Y_k = \left[\overline{P}_k, \overline{Q}_r^{(k)}, \overline{U}_r^{(k)}, \overline{U}_\theta^{(k)}, \overline{\Sigma}_{rr}^{(k)}, \overline{\Sigma}_{r\theta}^{(k)}\right]^t \tag{25}$$

where the exponent t is for the transposition of a vector; the index k and the exponent (k) denote the mechanical fields that are associated with the kth layer. The Laplace transformation of the pore pressure, fluid flow rate, radial and tangent displacements and radial and shear stresses in the kth layer are noted by $\overline{P}_k, \overline{Q}_r^{(k)}, \overline{U}_r^{(k)}, \overline{U}_\theta^{(k)}$, $\overline{\Sigma}_{rr}^{(k)}$ and $\overline{\Sigma}_{r\theta}^{(k)}$. The introduction of the vector $\boldsymbol{Y}_k$ is useful for the consideration of the boundary conditions and the continuity conditions at the interface between the layers as will be detailed after. It can be expressed in terms of a dot product between a 6×6 matrix $\mathcal{I}_k(r)$ and a vector of six constants that is defined by $\boldsymbol{X}_k = [A_k, B_k, C_k, D_k, E_k, F_k]^t$ as

$$\boldsymbol{Y}_k(r) = \mathcal{I}_k(r).\boldsymbol{X}_k \tag{26}$$

where the matrix $\mathcal{I}^{(k)}(r)$ is determined for each radial coordinate r in kth layer as

$$\mathcal{I}_k(r) = \begin{bmatrix} I_2(\xi_k) & K_2(\xi_k) & -M_k b_k r^2 & -\frac{M_k b_k}{r^2} & 0 & 0 \\ -\beta_k\left(I_1(\xi_k) - \frac{2I_2(\xi_k)}{\xi_k}\right) & \beta_k\left(K_1(\xi_k) + \frac{2K_2(\xi_k)}{\xi_k}\right) & 2\beta_k M_k b_k r & -\frac{2\beta_k M_k b_k}{r^3} & 0 & 0 \\ \delta_k\left(I_1(\xi_k) - \frac{2I_2(\xi_k)}{\xi_k}\right) & -\delta_k\left(K_1(\xi_k) + \frac{2K_2(\xi_k)}{\xi_k}\right) & -\frac{(H_k+M_k b_k^2-2G_k)r^3}{6G_k} & -\frac{H_k+M_k b_k^2}{2G_k r} & \frac{1}{r^3} & r \\ -\frac{2\delta_k I_2(\xi_k)}{\xi_k} & -\frac{2\delta_k K_2(\xi_k)}{\xi_k} & \frac{(H_k+M_k b_k^2-G_k/2)r^3}{3G_k} & \frac{1}{2r} & \frac{1}{r^3} & -r \\ -\theta_k\left(\frac{I_1(\xi_k)}{\xi_k} - \frac{6I_2(\xi_k)}{\xi_k^2}\right) & \theta_k\left(\frac{K_1(\xi_k)}{\xi_k} + \frac{6K_2(\xi_k)}{\xi_k^2}\right) & 0 & 2\left(H_k + M_k b_k^2 - G_k\right)\frac{1}{r^2} & -\frac{6G_k}{r^4} & 2G_k \\ 2\theta_k\left(-\frac{I_1(\xi_k)}{\xi_k} + \frac{3I_2(\xi_k)}{\xi_k^2}\right) & 2\theta_k\left(\frac{K_1(\xi_k)}{\xi_k} + \frac{3K_2(\xi_k)}{\xi_k^2}\right) & \left(H_k + M_k b_k^2 - G_k\right)r^2 & \frac{H_k+M_k b_k^2-G_k}{r^2} & -\frac{6G_k}{r^4} & -2G_k \end{bmatrix} \tag{27}$$

with

$$\xi_k = r\sqrt{s/c_k}$$

and $I_1(\xi)$, $I_2(\xi)$, $K_1(\xi)$ and $K_2(\xi)$ are the modified Bessel functions of the first and second kinds. The matrix $\mathcal{I}_k(r)$ can be determined by using Eq. (27) for any point with radial coordinate r inside the kth layer with given five poroelastic parameters that are the drained moduli H_k and G_k, the Biot's parameters b_k and M_k, and the

permeability κ_k. The parameters β_k, δ_k, θ_k and the diffusion coefficient c_k can be determined from the five given poroelastic parameters by using Eqs. (11) and (7).

The constants $\boldsymbol{X}_k$ of the cylindrical layers can be determined by solving the boundary and the continuity conditions. Once they are determined, the pore pressure, the radial and tangent displacements and the radial and shear stresses in each cylindrical layer can be obtained by Eq. (26). The tangent stress in the kth layer can be also calculated by Eq. (48) (see Appendix 1).

2.5 *Determination of* $\boldsymbol{X}_k$

To completely determine the poromechanical fields in the whole heterogeneous medium that is composed of N cylindrical layer, it is required to determine $6N$ constants that are A_k, B_k, C_k, D_k, E_k and F_k with k from 1 to N. This can be done by solving a system of $6N$ equations including the 6 boundary conditions at the inner and outer faces of the medium and $6(N-1)$ continuity conditions at $(N-1)$ interfaces between the layers. In each of the inner and outer faces, there are three boundary conditions that are the hydraulic condition (fluid pressure or fluid flow rate) and two mechanical conditions (radial and shear stresses or radial and tangent displacements). Besides, the poroelastic fields at an interface between two neighbor cylindrical layers must satisfy a system of six continuity conditions that can be combined in the following vector form: $\boldsymbol{Y}_k(r_k) = \boldsymbol{Y}_{k+1}(r_k)$ where the vector $\boldsymbol{Y}_k$ contains six components as defined by Eq. (25). This condition yields

$$\left[\mathcal{I}_k(r_k) \; -\mathcal{I}_{k+1}(r_k)\right]\begin{bmatrix}\boldsymbol{X}_k\\ \boldsymbol{X}_{k+1}\end{bmatrix} = 0 \tag{28}$$

where r_k is the radial coordinate of the interface between a kth and $(k+1)$th layers.

Considering for example a case with radial and shear stresses applied on the inner boundary of the hollow cylinder as described by Eq. (1). The outer boundary is fixed in displacement. Pore pressure is nil on both boundaries. These boundary conditions can be expressed as

$$\begin{bmatrix}\mathcal{I}_1(r_{in})[1]\\ \mathcal{I}_1(r_{in})[5]\\ \mathcal{I}_1(r_{in})[6]\end{bmatrix}\boldsymbol{X}_1 = \begin{bmatrix}0\\ \tilde{\sigma}_{in}\\ \overline{\tau}_{in}\end{bmatrix} \tag{29}$$

and

$$\begin{bmatrix}\mathcal{I}_N(r_{out})[1]\\ \mathcal{I}_N(r_{out})[3]\\ \mathcal{I}_N(r_{out})[4]\end{bmatrix}\boldsymbol{X}_N = \begin{bmatrix}0\\ 0\\ 0\end{bmatrix} \tag{30}$$

where $\tilde{\sigma}_{in}$ and $\overline{\tau}_{in}$ are the Laplace transforms of the radial and shear stresses that are applied on the inner boundary of the hollow cylinder; $\mathcal{I}_1(r_{in})[1]$, $\mathcal{I}_1(r_{in})[5]$ and $\mathcal{I}_1(r_{in})[6]$ are the first, fifth and sixth rows of $\mathcal{I}_1(r_{in})$; $\mathcal{I}_1(r_{out})[1]$, $\mathcal{I}_1(r_{out})[3]$ and $\mathcal{I}_1(r_{out})[4]$ are the first, third and fourth rows of $\mathcal{I}_N(r_{out})$. The combination of the Eqs. systems (28) (with k from 1 to $N-1$), (29) and (30) forms a system of $6n$ Eqs. that can be represented in the following matrix form

$$\boldsymbol{M}\cdot\boldsymbol{X} = \boldsymbol{F} \tag{31}$$

where $\boldsymbol{X}$ is the vector of $6N$ constants A_k, B_k, C_k, D_k, E_k and F_k with k from 1 to N: $\boldsymbol{X} = [A_1, B_1, C_1, D_1, E_1, F_1, \ldots, A_N, B_N, C_N, D_N, E_N, F_N]^t$; $\boldsymbol{F}$ is the vector of the poroelastic loadings at the inner and outer boundaries. For the considering example of radial and shear stresses applied on the inner

Table 1 Input parameters for the numerical examples

H_0 (GPa)	G_0 (GPa)	M_0 (GPa)	b_0	κ_0 (m^2/Pa/s)
20	10	18	0.7	10^{-18}

boundary, $\boldsymbol{F}$ can be expressed as: $\boldsymbol{F} = \left[0, \tilde{\sigma}_{in}, \overline{\tau}_{in}, 0, \ldots, 0\right]^t$. The matrix $\boldsymbol{M}$ can be constructed from the matrix $\mathcal{I}_k$ of the cylindrical layers as

$$\boldsymbol{M} = \begin{bmatrix} \mathcal{I}_1(r_{in})[1] & \ldots & 0 & 0 & \ldots & 0 & 0 \\ \mathcal{I}_1(r_{in})[5] & \ldots & 0 & 0 & \ldots & 0 & 0 \\ \mathcal{I}_1(r_{in})[6] & \ldots & 0 & 0 & \ldots & 0 & 0 \\ 0 & \ldots & 0 & 0 & \ldots & 0 & \mathcal{I}_N(r_{out})[1] \\ 0 & \ldots & 0 & 0 & \ldots & 0 & \mathcal{I}_N(r_{out})[3] \\ 0 & \ldots & 0 & 0 & \ldots & 0 & \mathcal{I}_N(r_{out})[4] \\ \mathcal{I}_1(r_1) & -\mathcal{I}_2(r_1) & 0 & 0 & \ldots & 0 & 0 \\ \ldots & \ldots & \ldots & \ldots & \ldots & \ldots & \ldots \\ 0 & \ldots & \mathcal{I}_k(r_k) & -\mathcal{I}_{k+1}(r_k) & \ldots & 0 & 0 \\ \ldots & \ldots & \ldots & \ldots & \ldots & \ldots & \ldots \\ 0 & \ldots & 0 & 0 & \ldots & \mathcal{I}_{n-1}(r_{n-1}) & -\mathcal{I}_n(r_{n-1}) \end{bmatrix} \tag{32}$$

We note that all the values in the first three rows of $\boldsymbol{M}$ are zeros except the six values in the first six columns; all the values in the 4th, 5th and 6th rows of $\boldsymbol{M}$ are zeros except the six values in the last six columns; all the values in the $(6\ k + 1)$th to $(6\ k + 6)$th rows with k from 1 to $N - 1$ are zeros except the twelve values in the $(6\ k\text{-}5)$th to $(6\ k + 6)$th columns. The matrix $\boldsymbol{M}$ depends only on the poroelastic properties and the radii of the cylindrical layers, and the vector $\boldsymbol{F}$ is constructed by only considering the boundary conditions. We note that the matrix $\boldsymbol{M}$ defined by Eq. (32) is constructed for the case of radial and shear stress applied on the boundary. But it can be employed for the cases with any boundary conditions with a minor modification. For example, if radial displacement is applied instead of the radial stress in the inner boundary, we just need to replace the 5th row of $\mathcal{I}_1(r_{in})$ by its 3th row, and so on. Knowing $\boldsymbol{M}$ and $\boldsymbol{F}$, we can compute the vector of the unknown constant $\boldsymbol{X}$ by: $\boldsymbol{X} = \boldsymbol{M}^{-1}.\boldsymbol{F}$. Once $\boldsymbol{X}$ is determined, the poromechanical fields in each local layer can be obtained by Eqs. (26) and (48). The solution in time space are obtained by the inverse Laplace transform using the Stehfest's method [13]. This method is chosen because of to its stability, fast convergence and easy to implement in a computation code.

3 Comparisons with existing results

We consider an example with power radial variations of the poroelastic properties as

$$\frac{H}{H_0} = \frac{G}{G_0} = \frac{M}{M_0} = \left(\frac{r}{r_{in}}\right)^{m_1}; \frac{b}{b_0} = \left(\frac{r}{r_{in}}\right)^{m_2}; \frac{\kappa}{\kappa_0} = \left(\frac{r}{r_{in}}\right)^{m_3} \tag{33}$$

where H_0, G_0, M_0, b_0 and κ_0 are certain reference parameters that are given in Table 1; m_1, m_2 and m_3 are the coefficients that define the radial variations of the poroelastic properties. The present model is not limited to an equal radiation of the elastic moduli H, G and the Biot's Modulus. But we consider this case in this example to make clearer the analysis. The homogeneous case corresponds to the case with $m_1 = m_2 = m_3 = 0$, and the poroelastic parameters are equal to the reference poroelastic parameters that are given in Table 1. Data given in Table 1 are typical properties of shale. They are considered just for the numerical examples and benchmark purpose. The hollow cylinder is subjected to pure shear loading (see Eq. (1)).

In some situation such as a wellbore in a petroleum reservoir, an interfacial transition zone around the grains in concrete, cortical bone or functionally graded composite, the material properties varies smoothly in the radial direction (see, e.g., [10]. In such a situation, the power approximation that is expressed by Eq. (34) is appropriate for describing the spatial distribution of the material properties.

Figure 2 shows a perfect coherence between the results of the present method and the ones of Detournay and Cheng [6] that were developed for a homogeneous cylindrical borehole: $m_1 = m_2 = m_3 = 0$ and $r_{out} \to \infty$. In this comparison, the diffusion time is fixed at one hour. The homogeneous poroelastic parameters used for the simulation are given in Table 1. The results are plotted in the nearby region of the borehole wall up to

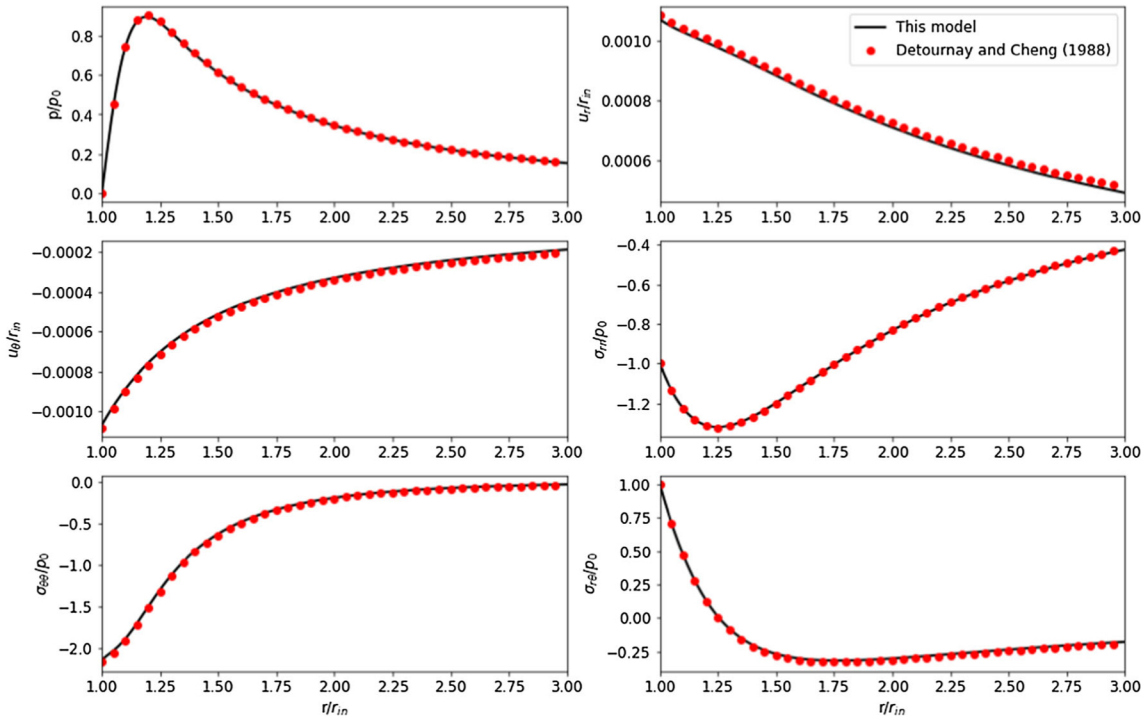

Fig. 2 A comparison of the present model and the solutions of Detournay and Cheng [6] that were developed for a homogeneous borehole. Results are obtained at $\theta = 0$

$r/r_{in} = 3$. The maximum pore pressure and compression radial stress are not located at the borehole wall bet in a nearby region. At one hour of diffusion, that region is located at $r/r_{in} = 1.25$. The absolute values of the radial and tangent displacements and the tangent stress are maximum at the borehole wall and tend to zero at infinity. The shear stress decreases from the applied value $\sigma_{r\theta}/p_0 = 1$ to a negative value at $r/r_{in} \approx 1.7$ and then tends to zero at the far-field region. This perfect agreement confirms the validity of the formula that is expressed in Eq. (27) at least for the case with $r_{out} \to \infty$. Unfortunately, results for the case with a bounded outer radius does not exist in the literature for a further validation of the transient diffusion situation.

To strengthen the validation of the developed method, another validation with radial variation of the poroelastic properties was considered. Jabbari et al. [10] developed analytical results for the steady state thermoelastic response of a functionally graded hollow cylinder that is subjected to a general loading condition. Their results can be adapted to an equivalent poroelastic problem at the steady state regime with pure shear loading by changing between the thermoelastic parameters and the poroelastic parameters. Also, it is required to reduce the considered general loading condition to a pure shear loading condition that is defined by Eq. (1). Such adaptation requires only a little effort and is not detailed in this paper. However, we should remark that there is a mistyping in the results of Jabbari et al. [10]: a factor $1/2$ was missing in their Eq. (51) that describe the shear stress $\sigma_{r\theta}$. The adapted results will be considered to validate the present method at a large diffusion time.

Figure 3 shows the distribution of the shear stress $\sigma_{r\theta}$ in the radial direction of a hollow cylinder with: $r_{in}/r_{out} = 2/3$. The poroelastic properties are defined by Eq. (33) with $m_1 = 2$, $m_2 = m_3 = 0$. The outer boundary is fixed in displacement, and the inner boundary is subjected to a pure shear loading as defined by Eq. (1). The results are given for different diffusion times that range from a short diffusion time of just one minutes to a very large diffusion time of 10^4 minutes that corresponds to a steady state regime. It can be observed that the shear stress decreases from the applied value $\sigma_{r\theta}/p_0 = 1$ at the borehole wall to 20% to 40% at the outer boundary depending on the diffusion time. The shear stress at the outer boundary is higher for a higher diffusion time. At a large diffusion time, the shear stress obtained by the present model matches perfectly with the analytical results that were derived by Jabbari et al. [10] at the steady state regime. The comparison of the present results and the reference results for other poromechanical fields is given in Figs. 4, 5, 6 and 7. These validations were obtained for the case with radial variations of the elastic moduli (H and G)

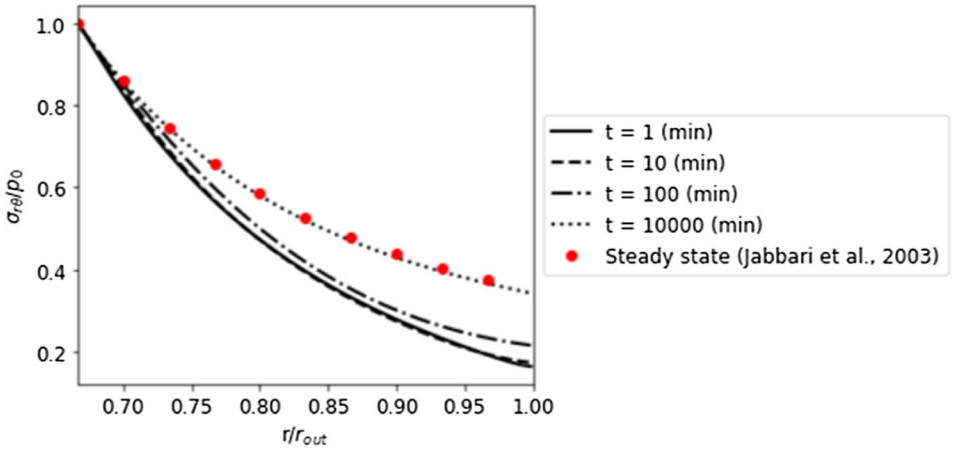

Fig. 3 Shear stress of a functionally graded hollow cylinder at different diffusion times with $m_1 = 2$, $m_2 = m_3 = 0$

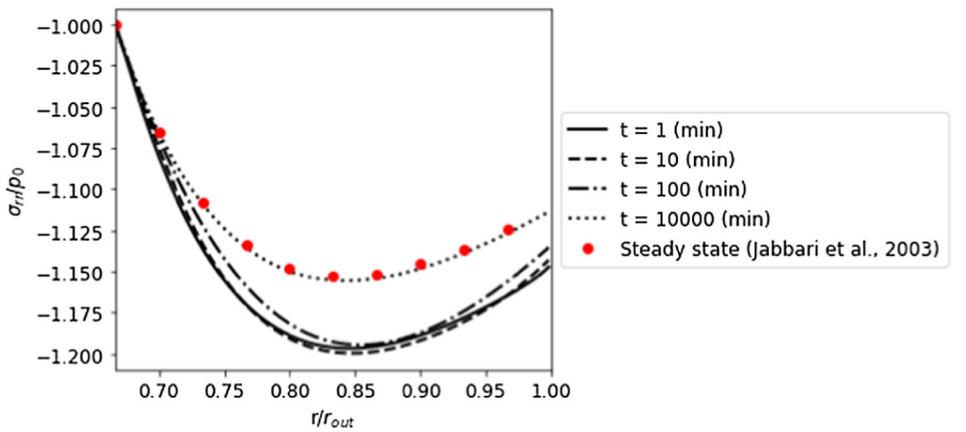

Fig. 4 Radial stress of a functionally graded hollow cylinder with $m_1 = 2$, $m_2 = m_3 = 0$

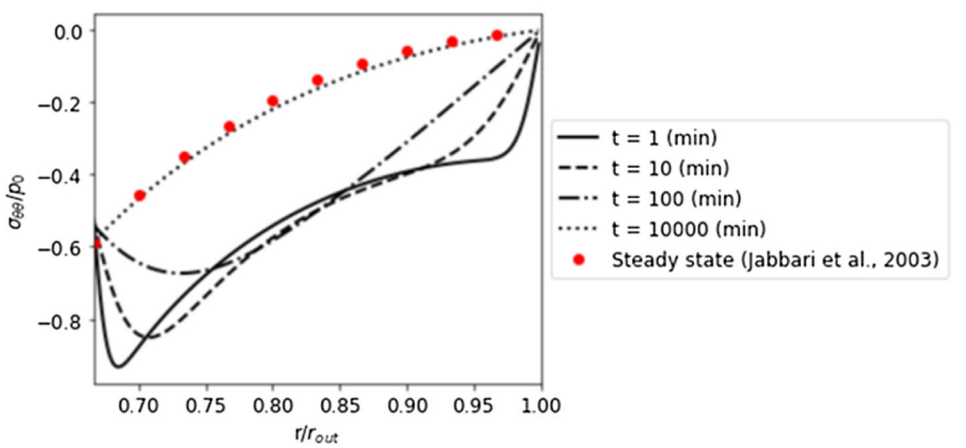

Fig. 5 Tangent stress of a functionally graded hollow cylinder with $m_1 = 2$, $m_2 = m_3 = 0$

and the Biot's modulus. But it is not limited to this case. Similar validations can be also obtained for the radial variation of the Biot's coefficient and the permeability.

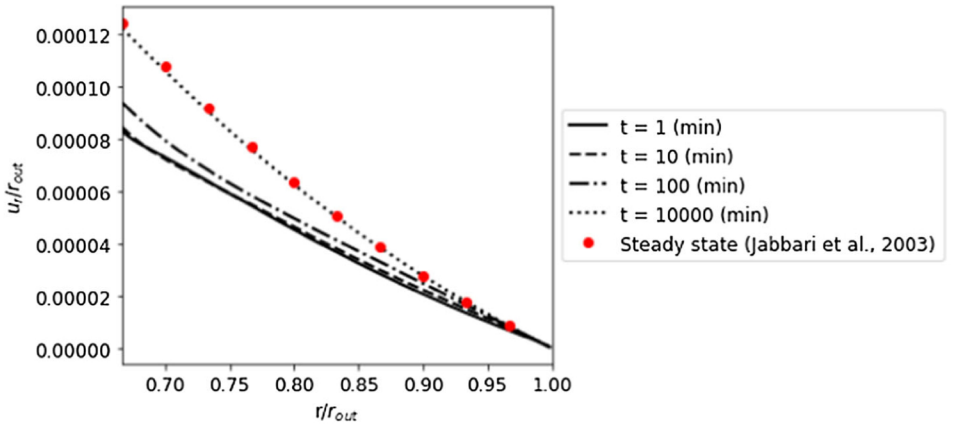

Fig. 6 Radial displacement of a functionally graded hollow cylinder with $m_1 = 2$, $m_2 = m_3 = 0$

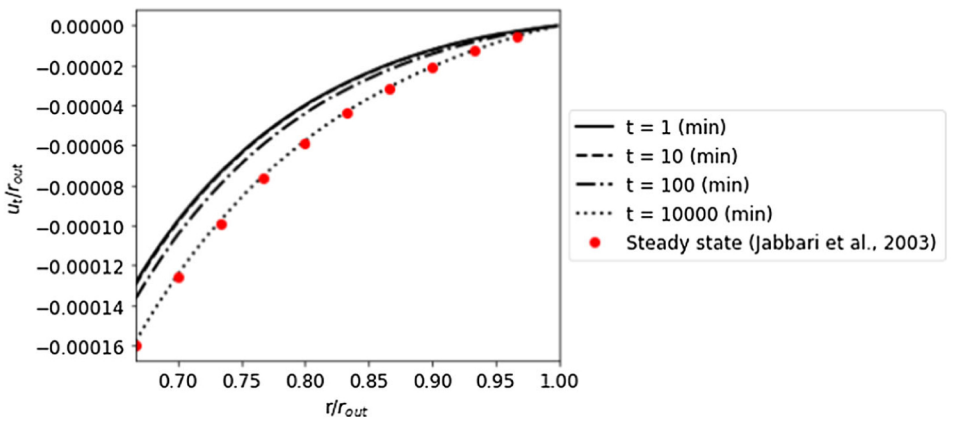

Fig. 7 Tangent displacement of a functionally graded hollow cylinder with $m_1 = 2$, $m_2 = m_3 = 0$

4 Sensitivity analysis

Let us consider the problem in which the results for the case with $m_1 = 2$ are shown in Figs. 3, 4, 5 and 7. To analyze the sensitivity of the heterogeneity on the poroelastic response of the hollow cylinder under a shear loading, the parameters m_1, m_2 and m_3 were allowed to vary in large ranges. The sensitivity of each parameter will be studied separately.

Figure 8 shows the results obtained for the sensitivity of m_1 that varies in a large range from -1 to 2. The Biot's coefficient and the permeability are assumed to be homogeneous in this case: $m_2 = m_3 = 0$. The diffusion time was fixed at 100 min and other parameters are given in Table 1. Pore pressure is nil at both inner and outer boundaries because of the boundary conditions. The radial distribution of pore pressure has a belly shape. The maximum pore pressure is in the zone close to the middle of the hollow cylinder. A higher value of m_1 corresponds to a higher pore pressure pic. The effects of m_1 on both the radial and tangent displacements are significant (Figs. 9 and 10). This dependency is quite monotonic because a higher value of m_1 corresponds to higher elastic moduli that leads to lower displacements at the inner boundary. The outer displacements are nil because of the considered boundary conditions.

Figure 11 shows a very interesting sensitivity of m_1 to the tangent stress. For $m_1 = -1$, $\sigma_{\theta\theta}$ increases monotonically from a compressive stress at the inner surface to zero at the outer surface where the displacements are blocked. This is not the case for a positive value of m_1. Indeed, with $m_1 = 1$ or 2, the minimum tangent stress is not at the inner surface of the hollow cylinder but at a region inside the hollow cylinder that is close to the inner surface. Dislike the case of the tangent stress, the effects of m_1 on the radial and shear stresses are almost negligible as shown in Figs. 12 and 13. This is because the radial and shear stresses are considered as boundary conditions that minimize the effect of the elastic moduli on these stress.

The sensitivity of the radial variation of the Biot's coefficient on the pore pressure is shown in Fig. 14. A large range of the parameter m_2 from -0.05 to 0.1 was considered. The dependence of the pore pressure on

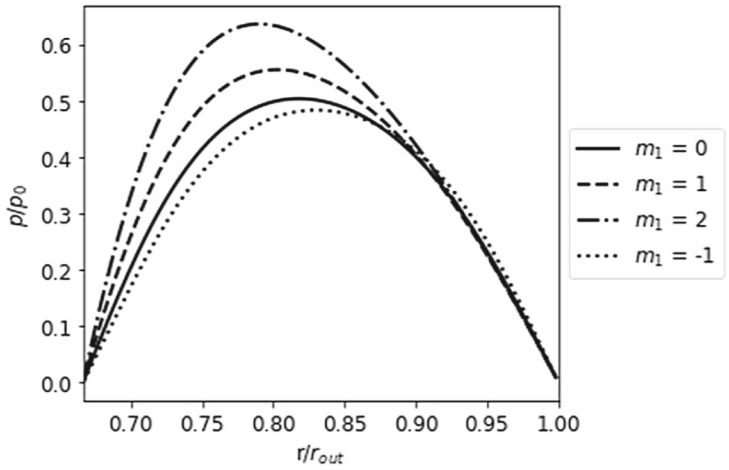

Fig. 8 Pore pressure distribution in the radial direction of a functionally graded hollow cylinder at 100 min of diffusion time: sensitivity of m_1

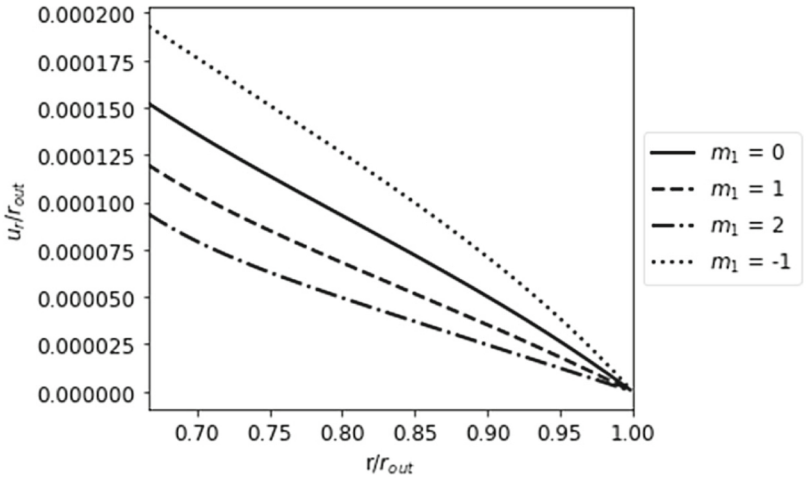

Fig. 9 Radial displacement of a functionally graded hollow cylinder: sensitivity of m_1

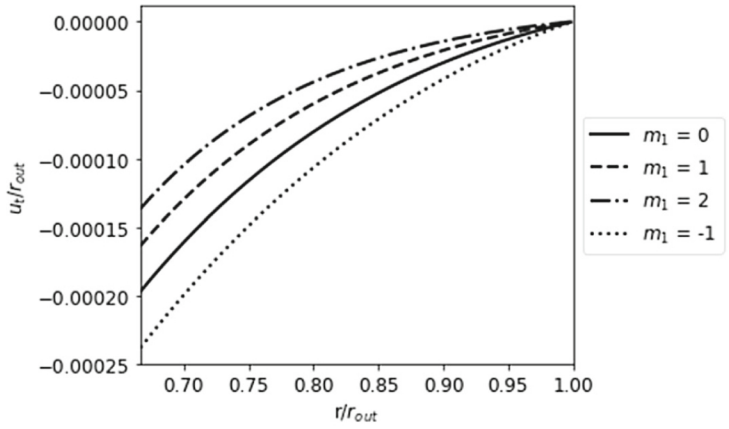

Fig. 10 Tangent displacement of a functionally graded hollow cylinder: sensitivity of m_1

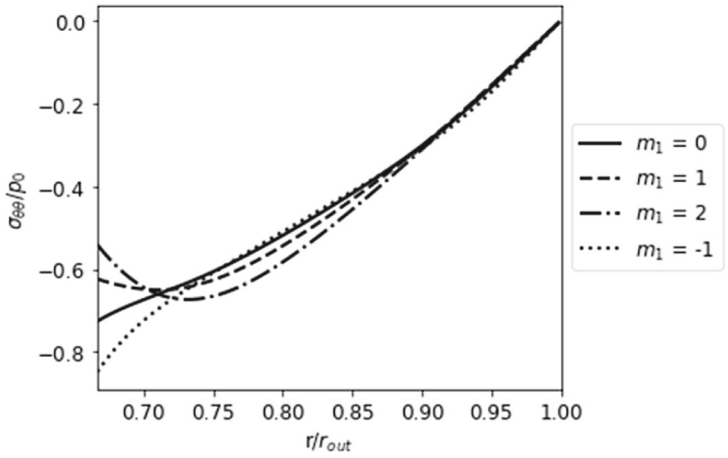

Fig. 11 Tangent stress of a functionally graded hollow cylinder: sensitivity of m_1

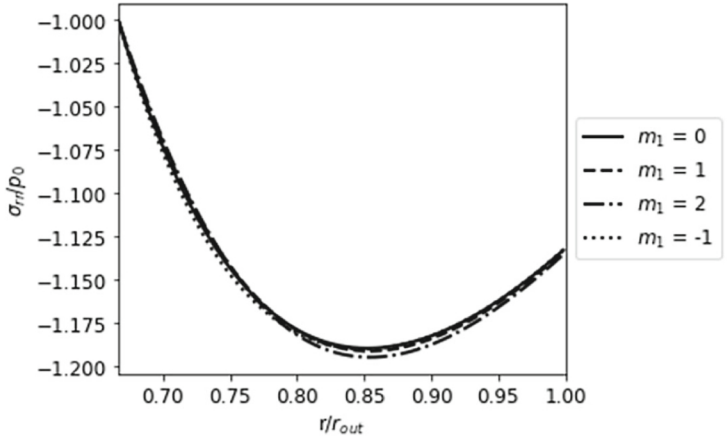

Fig. 12 Radial stress of a functionally graded hollow cylinder sensitivity of m_1

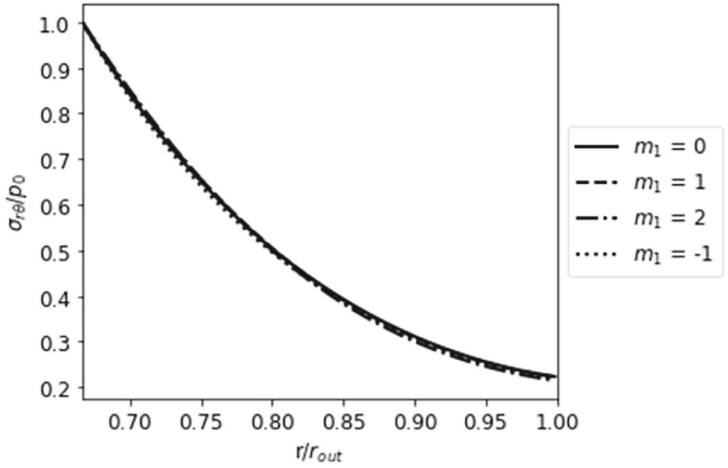

Fig. 13 Shear stress of a functionally graded hollow cylinder sensitivity of m_1

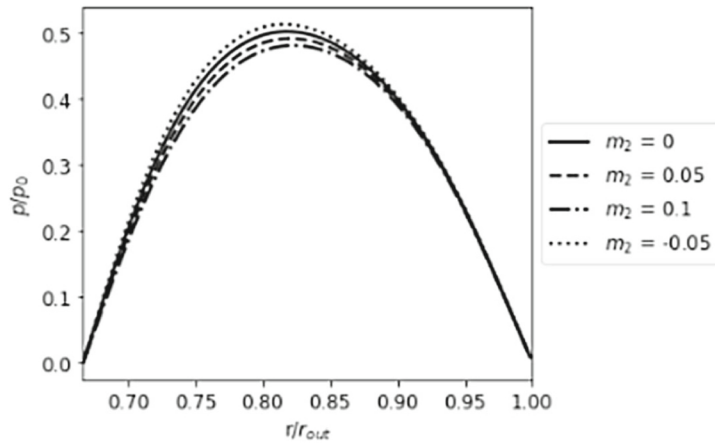

Fig. 14 Pore pressure distribution in the radial direction of a functionally graded hollow cylinder at 100 min of diffusion time: sensitivity of m_2

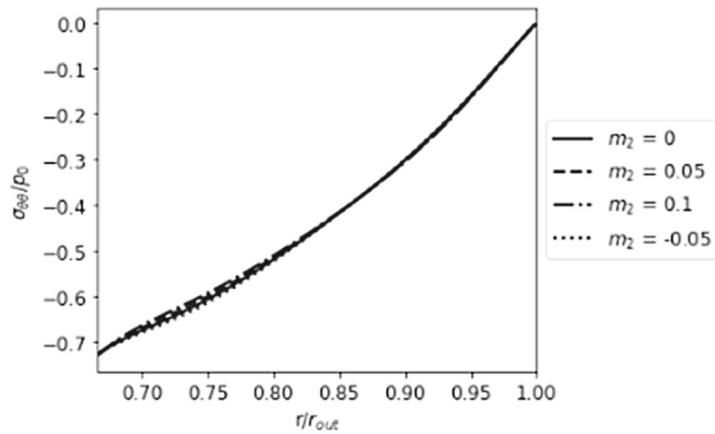

Fig. 15 Tangent stress of a functionally graded hollow cylinder: sensitivity of m_2

m_2 is not significant even at the middle of the hollow cylinder. The effect of m_2 is also negligible for the other poromechanical fields (see, e.g., Fig. 15). Such negligible Biot's effect is naturally expected for a pure shear loading condition that is considered herein.

Inversely, a very strong sensitivity of the results to the parameter m_3 was observed (Fig. 16). In this example, homogeneous elastic moduli and homogeneous Biot's modulus and coefficient were considered: $m_1 = m_2 = 0$. Only the permeability is assumed to vary radially. The pore pressure profile changes significantly while changing the parameter in a range from -2 to 3.

It has a convex shape for most of the cases, but its shape can become concave for a high value of $m_3 = 3$. Such significant effect manifests also for other poromechanical fields as shown in Fig. 17, 18, 19, 20 and 21. In particular, the permeability heterogeneity strongly influences the shape of the tangent stress (Fig. 19).

Figure 22 shows the results obtained for the pore pressure distribution in a thin hollow cylinder with $r_{in} = 0.09$ (m) and $r_{out} = 0.1$ (m). The heterogeneous parameters are $m_1 = 2$, $m_2 = 0.1$ and $m_3 = -2$. Pore pressure tends to zero at a large diffusion time. However, pore pressure at the middle of the cylinder is very high at a short diffusion time. It reaches almost $2/3$ of the applied shear stress at one to ten minutes of diffusion. The tangent stress has also a quite similar shape with a high compressive value at the middle of the cylinder (Fig. 23).

5 Conclusions

The poroelastic response of a functionally graded hollow cylinder subjected to an asymmetric loading condition was modeled by a multilayer technique. Analytical solutions in the transformed Laplace space were obtained for each layer. The results in Laplace space of the whole medium are obtained by considering the continuity

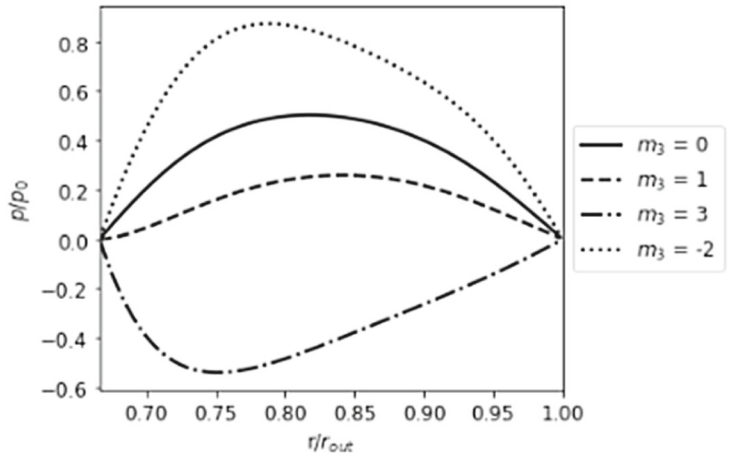

Fig. 16 Pore pressure distribution in the radial direction of a functionally graded hollow cylinder at 100 min of diffusion time: sensitivity of m_3

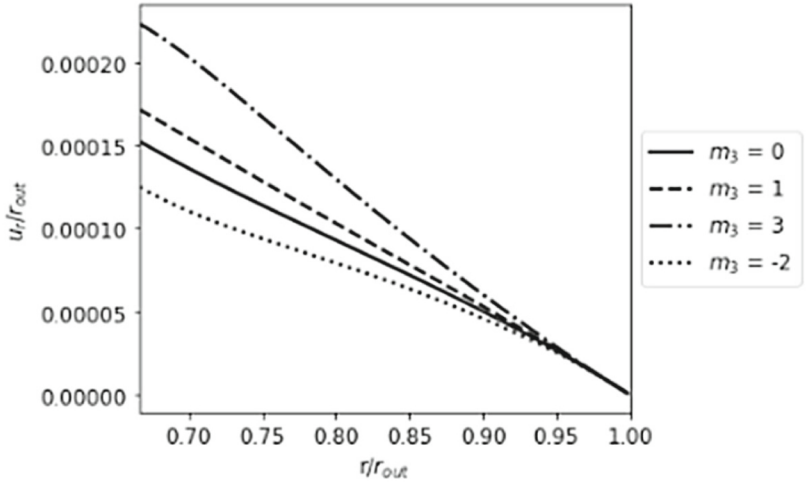

Fig. 17 Radial displacement of a functionally graded hollow cylinder: sensitivity of m_3

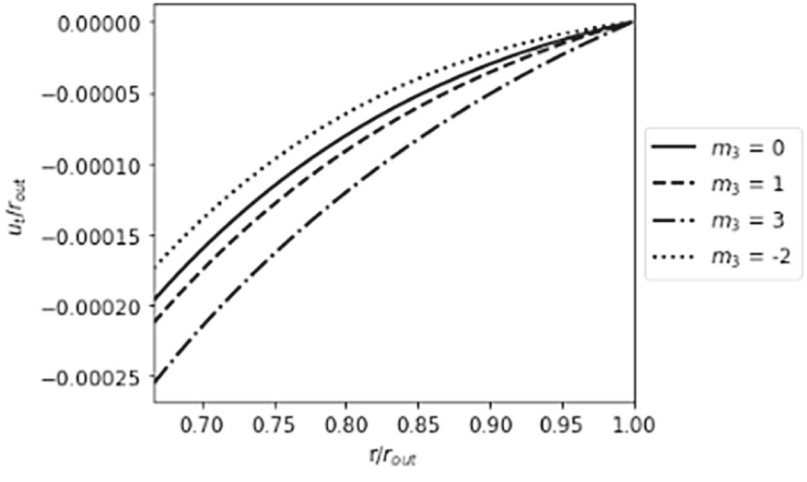

Fig. 18 Tangent displacement of a functionally graded hollow cylinder: sensitivity of m_3

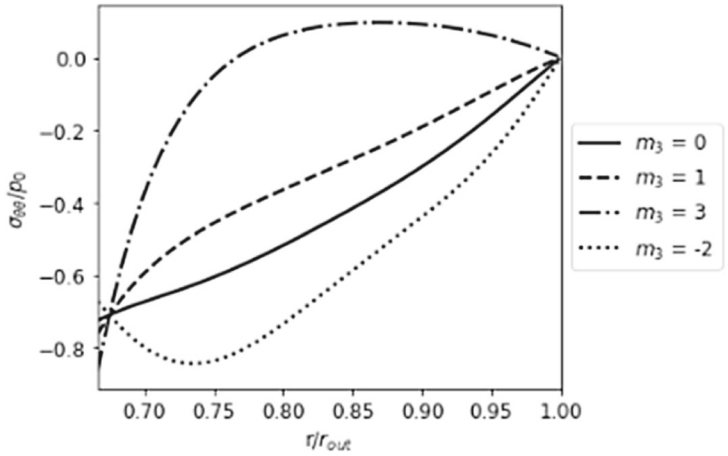

Fig. 19 Tangent stress of a functionally graded hollow cylinder: sensitivity of m_3

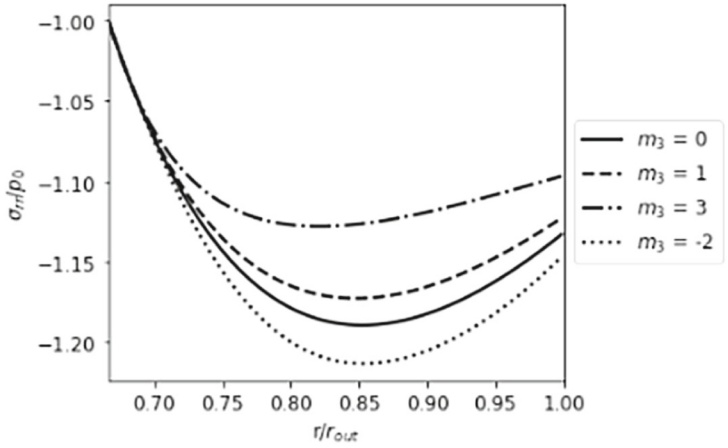

Fig. 20 Radial stress of a functionally graded hollow cylinder: sensitivity of m_3

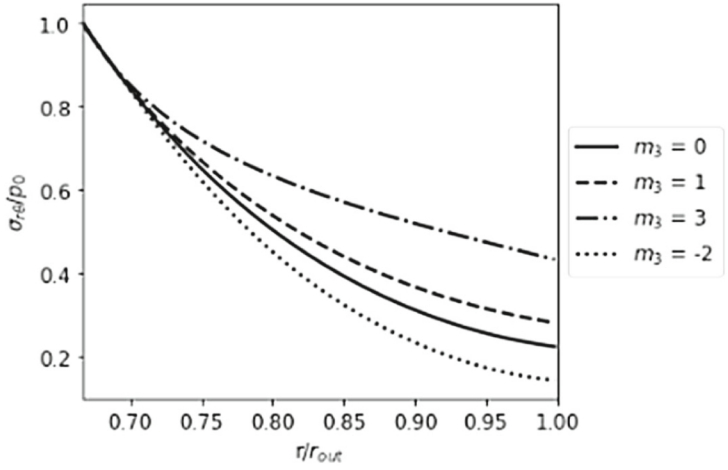

Fig. 21 Shear stress of a functionally graded hollow cylinder: sensitivity of m_3

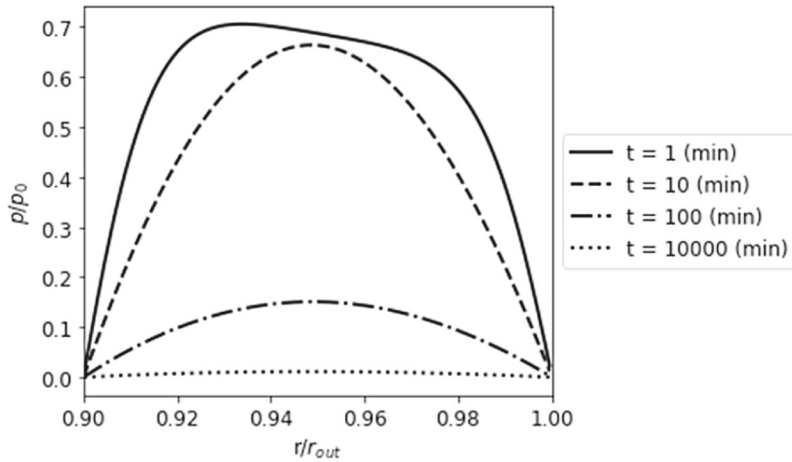

Fig. 22 Pore pressure of a thin hollow cylinder with $m_1 = 2$, $m_2 = 0.1$ and $m_3 = -2$

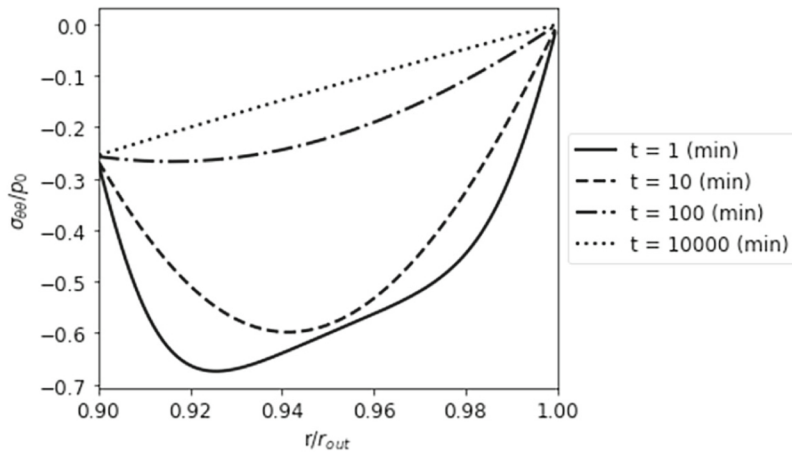

Fig. 23 Tangent stress of a thin hollow cylinder with $m_1 = 2$, $m_2 = 0.1$ and $m_3 = -2$

condition at the interface between the layers. The results in time space were obtained by using the Stehfest's numerical method for the inverse Laplace transformation.

The obtained results were compared with existing results for both the homogeneous case with transient fluid diffusion and the steady state case with radial variations of the poroelastic properties. Perfect agreements between the results given by the present method and the references ones were obtained.

Sensitivity analysis were realized to clarify the influence of the heterogeneous parameters on the poroelastic response of the hollow cylinder. Significant influence of the radial variations of the elastic moduli, the Biot's modulus and the permeability was observed. However, the sensitivity of the results to the Biot's coefficient is negligible which is naturally expected for this pure shear loading case. The results obtained in this study can be applied to offer potential applications for many fields such as: study the poroelastic response of a cortical bone in biomechanics; study the poroelastic response of a borehole or a core sample in geomechanics; stability of a tunnel in geotechnics, etc.

Acknowledgements This research is funded by Vietnam National Foundation for Science and Technology Development (NAFOSTED) under grant number 107.02-2016.12.

Declaration

Conflict of interest We wish to confirm that there are no known conflicts of interest associated with this publication and there has been no significant financial support for this work that could have influenced its outcome.

Appendix 1: Detail development of the poromechanical fields in the Laplace space

The Laplace transform of the diffusion Eq. (17) is

$$\xi_k^2 \frac{\partial^2 \overline{Z}_k}{\partial \xi_k^2} + \xi_k \frac{\partial \overline{Z}_k}{\partial \xi_k} - \left(\xi_k^2 + 4\right)\overline{Z}_k = 0 \tag{34}$$

where s is the Laplace variable and the overbar stands for a variable in Laplace's space. The normalized fluid exchange in the transformed space that is the solution of the ordinary differential Eq. (34) can be expressed in term of the modified Bessel functions of the first and second kinds as

$$\overline{Z}_k = A_k I_2(\xi_k) + B_k K_2(\xi_k) \tag{35}$$

where I and K are the modified Bessel functions of the first and second kinds, respectively; the coefficients A_k and B_k are independent of the radial coordinate; the parameter ξ_k is defined by

$$\xi_k = r\sqrt{\frac{s}{c_k}} \tag{36}$$

Knowing the fluid exchange, other mechanical variables can be easily obtained by regarding the governing Eqs. Indeed, for each layer with homogeneous poroelastic properties, the following elegant relation can be obtained by combining Eqs. (20) to (24)

$$\frac{\partial\left(\overline{E}_k - \frac{b_k}{H_k}\overline{Z}_k\right)}{\partial r} = \frac{2G_k}{H_k + M_k b_k^2}\frac{2\overline{W}_k}{r} \tag{37}$$

and

$$\frac{2G_k}{H_k + M_k b_k^2}\frac{\partial \overline{W}_k}{\partial r} = \frac{2\left(\overline{E}_k - \frac{b_k}{H_k}\overline{Z}_k\right)}{r} \tag{38}$$

This differential equation system can be easily solved for two variables $\overline{W}_k$ and $\overline{E}_k - \frac{b_k}{H_k}\overline{Z}_k$ that yields

$$\overline{E}_k = \frac{b_k}{H_k} A_k I_2(\xi_k) + \frac{b_k}{H_k} B_k K_2(\xi_k) + C_k r^2 + D_k \frac{1}{r^2} \tag{39}$$

and

$$\overline{W}_k = \frac{H_k + M_k b_k^2}{2G_k}\left(C_k r^2 - D_k \frac{1}{r^2}\right) \tag{40}$$

Using the results that are expressed by Eqs. (35) and (39), it is now possible to calculate the transformed pore pressure using the Laplace transformation of the Biot's Eq. (24) as

$$P_k = I_2(\xi_k)A_k + K_2(\xi_k)B_k - M_k b_k r^2 C_k - \frac{M_k b_k}{r^2} D_k \tag{41}$$

The corresponding radial flow rate is

$$\begin{aligned} Q_r^{(k)} = &-\beta_k\left(I_1(\xi_k) - \frac{2I_2(\xi_k)}{\xi_k}\right)A_k + \beta_k\left(K_1(\xi_k) + \frac{2K_2(\xi_k)}{\xi_k}\right)B_k \\ &+ 2\beta_k M_k b_k r C_k - \frac{2\beta_k M_k b_k}{r^3} D_k \end{aligned} \tag{42}$$

The transformed radial and tangent displacements can be obtained regarding its relationship with the transformed volumetric strain and the rotational coefficient W as

$$\frac{1}{r^3}\frac{\partial}{\partial r}\left[r^3\left(U_r^{(k)} + U_\theta^{(k)}\right)\right] = E_k + 2W_k \tag{43}$$

$$r\frac{\partial}{\partial r}\left[\frac{1}{r}\left(U_r^{(k)} - U_\theta^{(k)}\right)\right] = E_k - 2W_k \tag{44}$$

where E_k and W_k are defined by Eqs. (39) and (40). Then the Laplace transformed radial and tangent displacements can be obtained by integrating the formulas (43) and (44) as

$$U_r^{(k)} = \delta_k\left(I_1(\xi_k) - \frac{2I_2(\xi_k)}{\xi_k}\right)A_k - \delta_k\left(K_1(\xi_k) + \frac{2K_2(\xi_k)}{\xi_k}\right)B_k - \frac{\left(H_k + M_k b_k^2 - 2G_k\right)r^3}{6G_k}C_k - \frac{H_k + M_k b_k^2}{2G_k r}D_k + \frac{1}{r^3}E_k + rF_k \tag{45}$$

and

$$U_\theta^{(k)} = -\frac{2\delta_k I_2(\xi_k)}{\xi_k}A_k - \frac{2\delta_k K_2(\xi_k)}{\xi_k}B_k + \frac{\left(H_k + M_k b_k^2 - G_k/2\right)r^3}{3G_k}C_k + \frac{1}{2r}D_k + \frac{1}{r^3}E_k - rF_k \tag{46}$$

The important properties of the modified Bessel functions given in Appendix 2 were considered to calculate the displacements. Once the transformed radial and tangent displacements are known, the transformed radial, tangent and shear strain components can be obtained via the strain–displacement relation (19). Then radial, tangent and shear stress can be obtained via the Laplace transformation of the constitutive Eqs. (22) and (23) as

$$\Sigma_{rr}^{(k)} = -\theta_k\left(\frac{I_1(\xi_k)}{\xi_k} - \frac{6I_2(\xi_k)}{\xi_k^2}\right)A_k + \theta_k\left(\frac{K_1(\xi_k)}{\xi_k} + \frac{6K_2(\xi_k)}{\xi_k^2}\right)B_k + 2\left(H_k + M_k b_k^2 - G_k\right)\frac{1}{r^2}D_k - \frac{6G_k}{r^4}E_k + 2G_k F_k \tag{47}$$

$$\Sigma_{\theta\theta}^{(k)} = \theta_k\left(\frac{I_1(\xi_k)}{\xi_k} - \frac{6I_2(\xi_k)}{\xi_k^2} - I_2(\xi_k)\right)A_k - \theta_k\left(\frac{K_1(\xi_k)}{\xi_k} + \frac{6K_2(\xi_k)}{\xi_k^2} + K_2(\xi_k)\right)B_k + 2\left(H_k + M_k b_k^2 - G_k\right)r^2 C_k + \frac{6G_k}{r^4}E_k - 2G_k F_k \tag{48}$$

$$\Sigma_{r\theta}^{(k)} = 2\theta_k\left(-\frac{I_1(\xi_k)}{\xi_k} + \frac{3I_2(\xi_k)}{\xi_k^2}\right)A_k + 2\theta_k\left(\frac{K_1(\xi_k)}{\xi_k} + \frac{3K_2(\xi_k)}{\xi_k^2}\right)B_k + \left(H_k + M_k b_k^2 - G_k\right)r^2 C_k + \frac{H_k + M_k b_k^2 - G_k}{r^2}D_k - \frac{6G_k}{r^4}E_k - 2G_k F_k \tag{49}$$

Appendix 2: Some properties of the modified Bessel functions

The following are some important properties of the modified Bessel functions that were considered in the development of the present results:

$$\int \frac{K_2(x)}{x}\mathrm{d}x = -\frac{K_1(x)}{x};\ \int \frac{I_2(x)}{x}\mathrm{d}x = \frac{I_1(x)}{x}$$

$$\int K_0(x)x\mathrm{d}x = -xK_1(x);\ \int I_0(x)x\mathrm{d}x = xI_1(x).$$

$$\int K_2(x)x^3\mathrm{d}x = -4x^2K_2(x) - x^3K_1(x);\ \int I_2(x)x^3\mathrm{d}r = -4x^2I_2(x) + x^3I_1(x)$$

$$K_0(x) = K_2(x) - \frac{2K_1(x)}{x};\ I_0(x) = I_2(x) + \frac{2I_1(x)}{x}$$

References

1. Abbas, I.A.: Generalized magneto-thermoelasticity in a nonhomogeneous isotropic hollow cylinder using the finite element method. Arch. Appl. Mech. **79**(1), 41–50 (2009)
2. Asgari, M., Akhlaghi, M.: Transient thermal stresses in two-dimensional functionally graded thick hollow cylinder with finite length. Arch. Appl. Mech. **80**(4), 353–376 (2010)
3. Atefi, G., Talaee, M.R.: Non-fourier temperature field in a solid homogeneous finite hollow cylinder. Arch. Appl. Mech. **81**(5), 569–583 (2011)
4. Biot, M.A.: General theory of three-dimensional consolidation. J. Appl. Phys. **12**(2), 155–164 (1941)
5. Cheng, A.H.D.: Poroelasticity, vol. 27. Springer, Cham (2016)
6. Detournay, E., Cheng, A.D.: Poroelastic response of a borehole in a non-hydrostatic stress field. Int. J. Rock Mech. Min. Sci. Geomech. Abst. **25**(3), 171–182 (1988)
7. Hervé, E., Zaoui, A.: Elastic behaviour of multiply coated fibre-reinforced composites. Int. J. Eng. Sci. **33**(10), 1419–1433 (1995)
8. Horgan, C.O., Chan, A.M.: The pressurized hollow cylinder or disk problem for functionally graded isotropic linearly elastic materials. J. Elast. **55**(1), 43–59 (1999)
9. Jabbari, M., Sohrabpour, S., Eslami, M.R.: Mechanical and thermal stresses in a functionally graded hollow cylinder due to radially symmetric loads. Int. J. Press. Vessels Pip. **79**(7), 493–497 (2002)
10. Jabbari, M., Sohrabpour, S., Eslami, M.R.: General solution for mechanical and thermal stresses in a functionally graded hollow cylinder due to nonaxisymmetric steady-state loads. J. Appl. Mech. **70**(1), 111–118 (2003)
11. Nguyen-Sy, T., Vu, M.N., Nguyen, T.K., Tran-Le, A.D., Nguyen, T.T.: Poroelastic behavior of a functionally graded hollow cylinder. In press (2020)
12. Rice, J.R., Cleary, M.P.: Some basic stress diffusion solutions for fluid-saturated elastic porous media with compressible constituents. Rev. Geophys. **14**(2), 227–241 (1976)
13. Stehfest, H.: Algorithm 368: Numerical inversion of Laplace transforms. Commun. ACM **13**(1), 47–49 (1970)